Polarized Light-Induced Molecular Orientation Control of Rigid Schiff Base Ni(II), Cu(II), and Zn(II) Binuclear Complexes as Polymer Composites

Hiroyuki Nakatori, Tomoyuki Haraguchi and Takashiro Akitsu *

Department of Chemistry, Faculty of Science, Tokyo University of Science, 1-3 Kagurazaka, Tokyo 162-8601, Japan; akitsulab@gmail.com (H.N.); haraguchi@rs.tus.ac.jp (T.H.)
* Correspondence: akitsu@rs.kagu.tus.ac.jp; Tel.: +81-3-5228-8271

check for updates

Abstract: We have investigated linearly polarized UV light-induced molecular orientation due to Weigert effect of composite materials of new six binuclear nickel(II), copper(II), and zinc(II) complexes of two rigid Schiff base ring ligands (**L$_1$** and **L$_2$**) composite materials with methyl orange (**MO**), an azo-dye, in polyvinylalchol (**PVA**) cast films. To compare the degree of molecular orientation, two ligands, namely flexible aliphatic cyclohexane (**ML$_1$**: **NiL$_1$**, **CuL$_1$**, **ZnL$_1$**) and rigid aromatic (**ML$_2$**: **NiL$_2$**, **CuL$_2$**, **ZnL$_2$**), were synthesized using amine moiety. We have also characterized these complexes by means of elemental analysis, IR, and UV-vis spectra, single crystal or powder X-ray diffraction (XRD) analysis, and so on. Composite materials of **ML$_1$** or **ML$_2$+MO+PVA** were also prepared to separately disperse the solutes in a polymer matrix. For any metal complexes, optical anisotropy (represented as the *R* parameters) of **ML$_2$+MO+PVA** was larger than **ML$_1$+MO+PVA** because of the rigidness of the ligands.
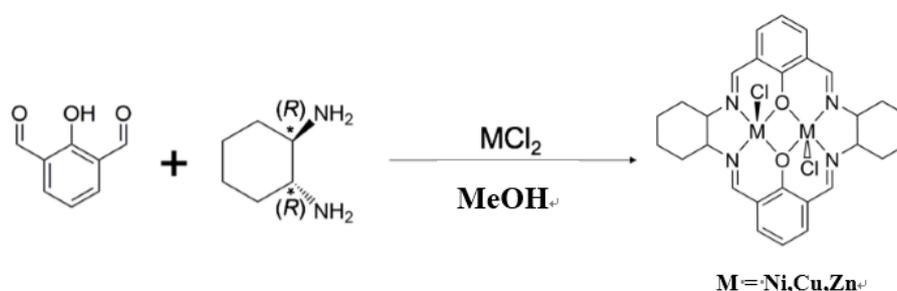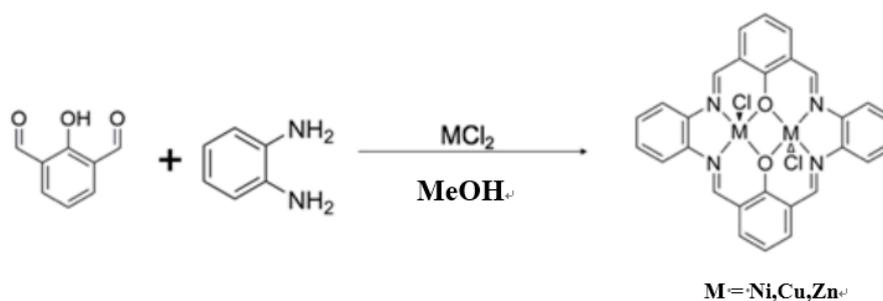
1. Introduction

Nowadays, specific *trans-cis* photoisomerization of photochromic azobenzene (**AZ**) and its related compounds are academically and commercially interesting and have been widely studied to date. Many industrial applications of photoisomerization have been reported in the fields such as molecular devices, molecular switches, polymers, and biochemistry, etc. [1–3]. In particular, *trans-cis* photoisomerization of AZ may also lead to the appearance of nonlinear optics, anisotropy (dichroism), and birefringence [4,5], which must be important features in the field of photofunctional materials. Additionally, it is also well-known that azo-compounds show molecular reorientation in polymers due to Weigert effect [6,7] (namely polarized light induces optical anisotropy of azo-compounds directly). When linearly polarized (UV, and vis under a certain condition), light continues to be irradiated to azo-compounds under a restricted environment to some extent; azo-compounds repeat photoisomerization and finally arrange in one direction that does not absorb linearly polarized light. By such mechanism and reason, molecular angular mobility, as well as birefringence and dichroism, also emerged due to azo-compound exhibiting *trans-cis* photoisomerization in a polymer matrix [8]. Many studies on orientation control based on the reorientation of azo-compounds have been reported so far.

The motivation of this work is to introduce such metal complexes into photosensitive polymer films, as follows. External (mechanical, electric, or magnetic) fields-induced molecular alignment of solutes in a matrix is a promising method for preparing switching or other functional materials

beyond single crystalline materials in solid states [9,10]. Classically, planar metal complexes (lowered symmetry from O_h to D_{4h}) may be an important example with which to elucidate their electronic states (assignment of d-d and π-π* transitions and other established associated electronic structures) by means of optical experiments such as polarized crystal (electronic) spectra [11]. However, spectral measurements for single crystals from a certain face (or along one or two axis) are not in agreement with plane-of-coordination-sphere molecular coordinates about d-orbitals symmetry due to orientation in the crystal packing of molecules. Thus, to overcome this experimental difficulty, alignment-tunable (or at least alignment-oriented) molecules of planer metal complexes may be preferable samples with which to study polarized spectral measurements. Moreover, such oriented metal complexes (e.g., $[CuCl_4]^{2-}$) in single crystals may also exhibit important other physical behavior such as thermochromism, as well as optical properties [12]. In this context, organic/inorganic hybrid materials of AZ and (planar) metal complexes deserve to be investigated by means of optical or other physical experiments. Organic/inorganic hybrid materials have the advantage of exhibiting additional electronic properties due to inorganic metal complexes, which is difficult for organic photofunctional polymers solely. However, light or laser (at the same time electric field) controlling of molecular alignment and its evaluation are not simple generally [13,14]. Based on the above-mentioned factors, we aimed to develop new functions and physical properties through the anisotropic arrangement of metal complexes that have azo-components in polymers. We have prepared organic/inorganic composite materials of methyl methacrylate (PMMA) polymer films separately that contain Schiff bases Ni(II), Cu(II), Zn(II) complexes, and AZ with various substituents [15–19]. In recent years, much effort has been devoted to controlling optical anisotropy using not AZ and PMMA but water-soluble methyl orange (MO) and polyvinyl alcohol (**PVA**) [20], by which application in protein systems may be also expected potentially. In this research, herein, as molecular design comparison from the viewpoint of receiving intermolecular interaction, we discuss the degree of induced optical anisotropy for binuclear complexes that have flexible cyclohexane moieties (**ML₁**) (Scheme 1) and more rigid aromatic phenyl moieties (**ML₂**) (Scheme 2) at the amine site.

Scheme 1. Preparation of **ML₁**.

Scheme 2. Preparation of **ML₂**.

2. Materials and Methods

2.1. Preparations of Complexes

All the reagents and solvents were of the highest commercial grade available (Aldrich, Wako, or TCI) were used as received without further purification. Those dissolved in methanol (20 mL), metal sources of chlorides (0.67 mmol), amines, and (*1R,2R*)-(−)-1,2-cyclohexanediamine for **L₁** or *o*-phenylenediamine for **L₂** (0.067 mmol) were refluxed for 1 day at room temperature to give rise to crude products. The solution was left overnight at room temperature. The resulting crude precipitates were filtered, thoroughly washed with methanol, and dried in vacuo. Only for **CuL₁**, the resulting precipitate was recrystallized in methanol and ethanol (1:1, *v/v*), taken in sample tube, and left alone for a few days to yield deep green single crystals suitable for single-crystal XRD analysis.

NiL₁: Yield: 21.8%. Anal. Found: C, 51.31%; H, 4.70%; N, 8.72%. Calcd. for $C_{28}H_{30}Cl_2N_4Ni_2O_2 \cdot H_2O$: C, 50.89%; H, 4.88%; N, 8.48%. IR(KBr); 1637 (s) (C=N), 1561 (s), 1481, 1446, 1334, 1236, 1055, 568(w), 3420(w) cm^{-1}.

CuL₁: Yield: 13.9%. Anal. Found: C, 50.54%; H, 4.63%; N, 8.59%. Calcd. for $C_{28}H_{30}Cl_2Cu_2N_4O_2 \cdot H_2O$: C, 50.15%; H, 4.81%; N, 8.36%. IR(KBr): 1626 (s) (C=N), 2364 (s), 2345(s), 1553, 1438, 1380, 1344, 1237, 1090, 1032, 889, 2930, 3434(w) cm^{-1}.

ZnL₁: Yield: 20.5%. Anal. Found: C, 51.25%; H, 4.61%; N, 8.54%. Calcd. for $C_{28}H_{30}Cl_2N_4O_2Zn_2$: C, 51.25%; H, 4.61%; N, 8.54%. IR(KBr): 1623 (s) (C=N), 1544, 1430, 1378, 1347, 1230, 1086, 1028, 884, 761, 2922, 3424(w) cm^{-1}.

NiL₂: Yield: 36.5%. Anal. Found: C, 61.04%; H, 2.88%; N, 9.87%. Calc. for $C_{28}H_{18}Cl_2N_4Ni_2O_2$: C, 53.32%; H, 2.88%; N, 8.88%. IR(KBr): 1625 (s) (C=N), 1536 (s), 1490, 1457, 1431, 1385, 1339, 1273, 1235, 1208, 1060, 909, 748, 3424 (w) cm^{-1}.

CuL₂: Yield: 32.7%. Anal. Found; C, 52.51%; H, 2.83%; N, 8.75%. Calcd. for $C_{28}H_{18}Cl_2Cu_2N_4O_2$: C, 52.51%; H, 2.83%; N, 8.75%. IR(KBr): 1620 (s) (C=N), 1530 (s), 1548, 1385, 1334, 1248, 1204, 1045, 755, 3459 (w) cm^{-1}.

ZnL₂: Yield: 32.7%. Anal. Found: C, 52.73%; H, 2.73%; N, 8.50%. Calcd. for $C_{28}H_{18}Cl_2N_4O_2Zn_2$: C, 52.21%; H, 2.82%; N, 8.70%. IR(KBr): 1623 (s) (C=N), 1552 (s), 1489, 1395, 1371, 1334, 1267, 1204, 1038, 760, 3451 (w) cm^{-1}.

2.2. Preparations of Composite Materials

Aqueous solutions of each complex (0.1 mM), **MO** (0.1 mM), and **PVA** (10 wt%) were mixed and cast onto a slide glass on the hot plate (333 K) for about 60 min to obtains cast films of the composite materials (**MLₙ+MO+PVA**).

2.3. Physical Measurements

Elemental analyses were carried out with a Perkin-Elmer 2400II CHNS/O analyzer Perkin-Elmer, Waltham, MA, USA) at Tokyo University of Science. Infrared (IR) spectra were recorded on a JASCO FT-IR 4200 spectrophotometer (JASCO, Tokyo, Japan) in the range of 4000–400 cm^{-1} at 298 K. (Polarized) electronic (UV-vis) spectra were measured on a JASCO V-650 spectrophotometer (JASCO, Tokyo, Japan) equipped with polarizer in the range of 800–220 nm at 298 K. Circular dichroism (CD) spectra were measured on a JASCO J-725 spectropolarimeter (JASCO, Tokyo, Japan) in the range of 800–200 nm at 298 K. Photo-illumination was carried out using a lamp (1.0 mW/cm²) with optical filters (UV λ = 200–400 nm), producing a sample using optical fibers and polarizer through optical filters.

2.4. X-ray Crystallography

Deep greenish prismatic single crystals of **CuL₁** were glued on top of a glass fiber and coated with a thin layer of epoxy resin to measure the diffraction data. Intensity data were collected on a Bruker APEX2 CCD diffractometer (Bruker, Billerica, MA, USA) with graphite-monochromated Mo Kα

radiation (λ = 0.7107 Å). Data analysis was carried out with a SAINT program package. The structures were solved by direct methods with a SHELXS-97, expanded by Fourier techniques, and refined by full-matrix least-squares methods based on F^2 using the program SHELXL-97 [21]. An empirical absorption correction was applied by a program SADABS. All non-hydrogen atoms were readily located and refined anisotropic thermal parameters. All hydrogen atoms were located at geometrically calculated positions and refined using riding models. Unfortunately, single crystals of the other complexes could not be obtained.

The powder X-ray diffraction patterns for **CuL$_2$** and **ZnL$_2$** were collected at 298 K on Rigaku Smart lab with CuKα radiation (λ = 1.5418 Å) at the University of Tokyo. Powder crystal structures were determined by means of Rietveld refinement using a Rigaku PDXL2 program package (Rigaku, Tokyo, Japan).

Crystallographic data for **CuL$_1$** (CCDC 1826446): $C_{28}H_{30}Cl_2Cu_2N_4O_2$, Orthorhombic, $P2_12_12$ (#18), Z = 4, a = 13.841(15) Å, b = 24.705(3) Å, c = 8.198(9) Å, V = 2803.2(6) Å^3, ρ_{calc} = 1.660 g/cm^3, μ = 1.775 mm^{-1}, F(000) = 1432.0, S = 0.765, $R_1[I>2\sigma(I)]$ = 0.0335, $wR2$ = 0.1096. Flack parameter = 0.014(10).

Crystallographic data for **CuL$_2$** (CCDC 1826434): $C_{28}H_{18}Cl_2Cu_2N_4O_2$, Triclinic, P-1 (#2), Z = 2, a = 7.750(4) Å, b = 8.460(4) Å, c = 15.256(7) Å, α = 85.59(12)°, β = 110.77(9)°, γ = 112.89(7)°, V = 2510(6) Å^3, R_{wp} = 5.28%.

Crystallographic data for **ZnL$_2$** (CCDC 1826435): $C_{28}H_{18}Cl_2N_4O_2Zn_2$ Triclinic, P-1 (#2), Z = 2, a = 13.87(4) Å, b = 14.56(4) Å, c = 13.18(4) Å, α = 85.19(15)°, β = 110.60(17)°, γ = 112.84(14)°, V = 2293(11) Å^3, R_{wp} = 4.25%. (See Supplementary Materials)

3. Results

3.1. Spectral Characterization

Figure 1 depicts CD spectra of chiral complexes (**ML$_1$**). As prepared using chiral amine, it could be confirmed that they are optically active products. Since these complexes afford identical structures except for metal ions, the spectral difference is attributed to transition associated with metal ions (d-d) or between metal and coordination atoms (CT) transitions mainly. The reason why the spectra in solutions are slightly different from that in solid state (KBr) may be artifact peaks due to LD components besides CD components [22].
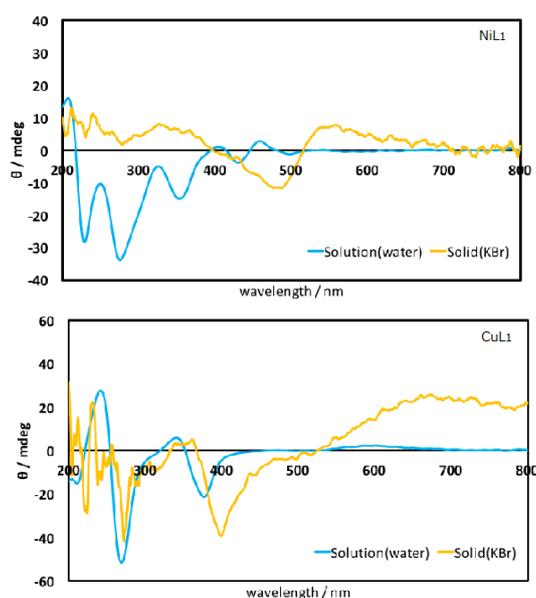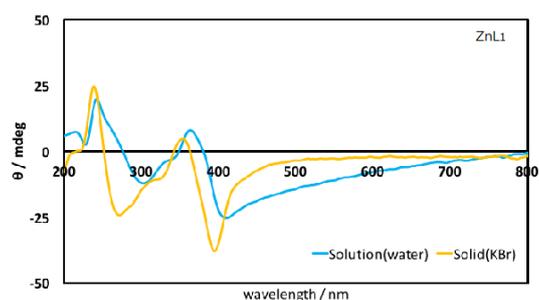

Figure 1. *Cont.*

Figure 1. CD spectra in aqueous solutions (blue) and KBr pellets (orange) for chiral complexes (**NiL₁**, **CuL₁**, and **ZnL₁**).

3.2. Structural Characterization

Figures 2–4 exhibits crystal structures of **CuL₁**, **CuL₂**, and **ZnL₂**, respectively. Each metal ion of binuclear chromophores affords a five-coordinated square pyramidal coordination geometry, in which metal ions are slightly lifted up towards the apical Cl atom from the [MN₂O₂] basal planes. Both apical Cl atoms are located on the opposite sides of a ligand plane in a symmetric manner. Rigidity of six-membered C ring derived from amines for **CuL₁** are **CuL₂** resulted in conformational difference of whole ligands. Besides them, most of bond lengths and angles are within common ranges of the analogous compounds [20].
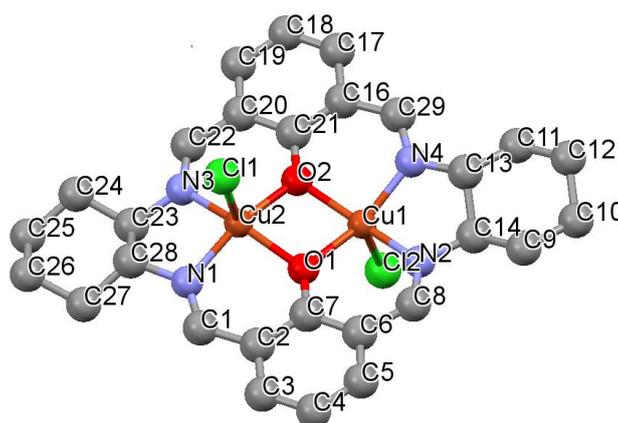

Figure 2. Crystal structures of **CuL₁** showing atom labeling schemes. Hydrogen atoms and crystalline water were omitted for clarity. Selected bond lengths [Å] and angles [°]: Cu1-N2 = 1.900(3), Cu1-O2 = 1.917(3), Cu1-N4 = 1.919(4), Cu1-O1 = 1.928(3), Cu1-Cl2 = 2.5297(13), Cu1-Cu2 = 2.9823(7), Cu2-N3 = 1.912(4), Cu2-N1 = 1.917(4), Cu2-O2 = 1.917(3), Cu2-O1 = 1.926(3), Cu2-Cl = 2.5290(13), N2-Cu1-O2 = 160.33(15), N2-Cu1-N4 = 89.07(15), O2-Cu1-N4 = 92.47(14), N2-Cu1-O1 = 92.97(14), O2-Cu1-O1 = 78.19(12), N4-Cu1-O1 = 157.03(15), N3-Cu2-N1 = 88.85(15), N3-Cu2-O2 = 92.52(14), N1-Cu2-O2 = 162.59(16), N3-Cu2-O1 = 155.27(15), N1-Cu2-O1 = 93.46(14), O2-Cu2-O1 = 78.23(12), Cu1-O2-Cu2 = 102.12(14), Cu2-O1-Cu1 = 101.42(13).
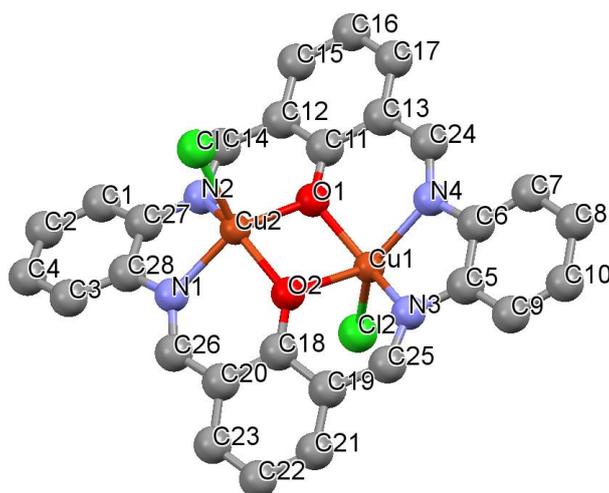
Figure 3. Crystal structures of **CuL₂** showing atom labeling schemes. Hydrogen atoms were omitted for clarity. Selected bond lengths [Å] and angles [°]: Cu1-Cu2 = 3.142(4), Cu1-Cl2 = 2.315(4), Cu2-Cl1 = 2.326(3), Cu1-O1 = 1.989(2), Cu1-O2 = 2.306(4), Cu2-O1 = 2.041(3), Cu2-O2 = 2.018(3), Cu1-N3 = 2.061(3), Cu1-N4 = 2.110(3), Cu2-N1 = 2.077(3), Cu2-N2 = 2.254(3), O1-Cu1-O2 = 78.53(9), O1-Cu2-O2 = 84.47(10), O1-Cu1-N3 = 140.88(9), O1-Cu1-N4 = 84.37(11), O2-Cu1-N3 = 77.09(12), O2-Cu1-N4 = 124.09(9), O2-Cu2-N2 = 140.00(9), O1-Cu2-N1 = 136.46(8), O1-Cu2-N2 = 78.62(14), O2-Cu2-N1 = 87.36(11), Cu1-O1-Cu2 = 102.45(9), Cu1-O2-Cu2 = 92.97(10).
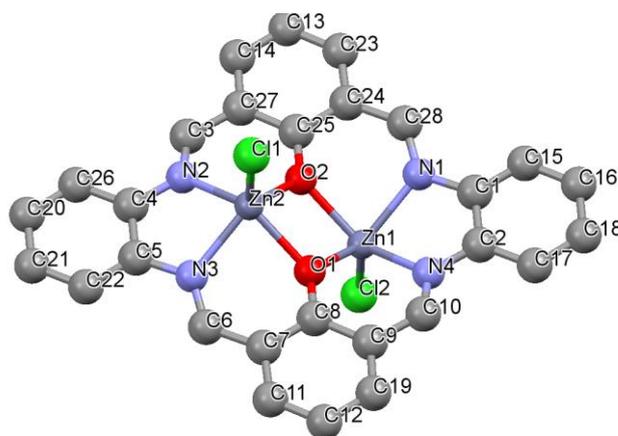

Figure 4. Crystal structures of **ZnL₂** showing atom labeling schemes. Hydrogen atoms were omitted for clarity. Selected bond lengths [Å] and angles [°]: Zn1-Zn2 = 3.244(10), Zn1-Cl2 = 2.250(5), Zn2-Cl1 = 2.250(5), Zn1-O1 = 1.998(7), Zn1-O2 = 2.120(5), Zn2-O1 = 2.120(5), Zn2-O2 = 1.998(7), Zn1-N1 = 2.151(6), Zn1-N4 = 2.231(6), Zn2-N2 = 2.231(6), Zn2-N3 = 2.151(6), O1-Zn1-O2 = 76.1(3), O1-Zn2-O2 = 76.1(3), O1-Zn1-N1 = 127.87(15), O1-Zn1-N4 = 82.8(2), O2-Zn1-N1 = 81.61(18), O2-Zn1-N4 = 130.50(15), O2-Zn2-N2 = 82.8(2), O1-Zn2-N2 = 130.51(15), O1-Zn2-N3 = 81.61(18), O2-Zn2-N3 = 127.88(15), Zn1-O1-Zn2 = 103.9(3), Zn1-O2-Zn2 = 103.9(3).

3.3. Linearly Polarized UV Light Induced Optical Anisotropy

At first, induced optical anisotropy was examined with polarized UV-vis spectra of **MO+PVA** and **MO+ML₁+PVA** (Table 1). Regarding the relative values (to 0 min) of an anisotropy parameter R (=$Abs_{0\text{deg}}/Abs_{90\text{deg}}$) [23], the parameters R increased with linearly polarized UV light irradiation time based on polarized UV-vis spectra (Figure 5). The anisotropy parameter before irradiation is set to 1 for simplicity. From the results, the parameters R increased with increasing irradiation time,

which implies that molecules were aligned in a direction to avoid absorbing polarized light. Thus, it is suggested that molecules are aligned in one direction, leading to a situation in which they cannot absorb irradiated polarized light furthermore [6]. Next, the corresponding data for **MO+ML$_2$+PVA** (Table 2) indicated that the maximum values of the anisotropy parameter for **MO+ML$_2$+PVA** (1.0279, 1.0222, and 1.0452 for **NiL$_2$**, **CuL$_2$**, and **ZnL$_2$**, respectively) are larger than those of **MO+ML$_1$+PVA** (0.9850, 1.0141, and 1.0230 for **NiL$_1$**, **CuL$_1$**, and **ZnL$_1$**, respectively), which expressed that **MO+ML$_2$+PVA** (incorporating more rigid aromatic ligands) are easier to align due to intermolecular interaction between **MO** and **ML$_2$** in **PVA** in which only **MO** is affected on Weigert effect directly [18,19].

Table 1. The relative *R* parameters for **MO+PVA** and **MO+ML$_1$+PVA** after linearly polarized UV light irradiation with detected wavelengths.

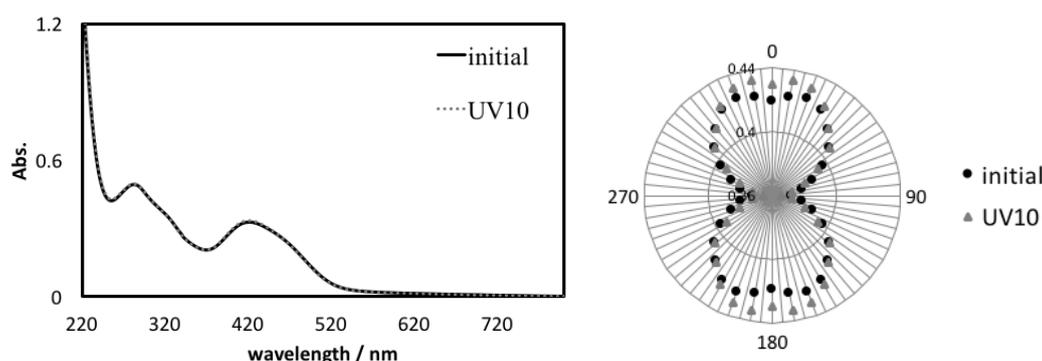| Time/min	MO+PVA n-π* 436 nm	MO+NiL$_1$+PVA π-π* 245 nm	MO+CuL$_1$+PVA π-π* 253 nm	MO+ZnL$_1$+PVA π-π* 242 nm
0	1	1	1	1
1	1.0208	0.9850	1.0141	1.0119
3	1.0311	0.9939	1.0033	1.0140
5	1.0382	0.9927	1.0055	1.0230
10	1.0459	0.9983	1.0049	1.0005

Figure 5. (**Left**) Polarized UV-vis spectra of ZnL$_2$+MO+PVA before and after 10 min polarized UV light irradiation. (**Right**) Polarizer angle dependence of absorbance of polarized UV-vis spectra (at 306 nm, π-π* band) of **ZnL$_2$+MO+PVA** before and after 10 min polarized UV light irradiation.
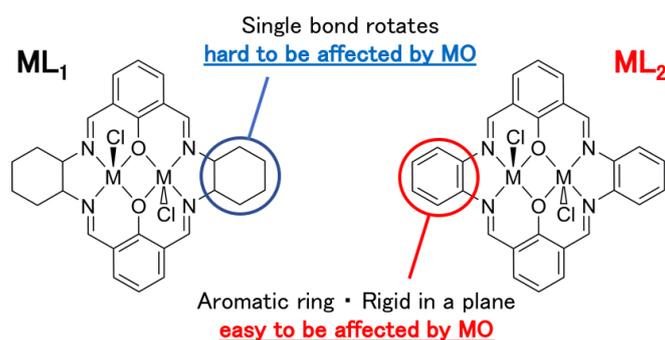
Table 2. The relative *R* parameters for **MO+ML$_2$+PVA** after linearly polarized UV light irradiation with detected wavelengths.

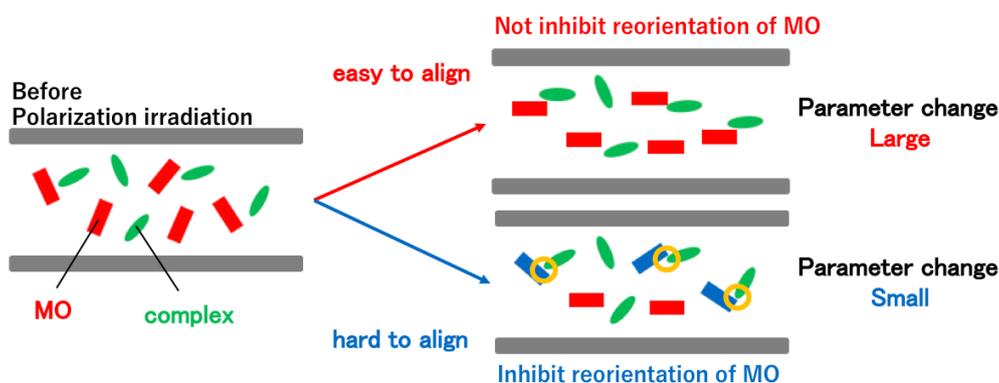| Time/min	MO+NiL$_2$+PVA π-π* 294 nm	MO+CuL$_2$+PVA π-π* 306 nm	MO+ZnL$_2$+PVA π-π* 306 nm
0	1	1	1
1	1.0082	1.0126	1.0223
3	1.0215	1.0109	1.0258
5	1.0130	1.0222	1.0382
10	1.0279	1.0192	1.0452

4. Discussion

Similar to the related study with theoretical analysis [24], explanation of the origin of the observed spectral changes in composite films can be also probed using Weigert effect for **MO** (as direct driving force) and intermolecular interaction to complexes in a polymer matrix. According to these results, the maximum change in the anisotropic parameter *R* was larger for **ML$_2$+MO+PVA** than **ML$_1$+MO+PVA** for all metals. From the results, it was found that **ZnL$_2$** in **ZnL$_2$+MO+PVA** is the

easiest to align. As a consideration, assumption summarized in Scheme 3 can be deduced. Flexibility is more important than chirality of ligand in this case [25]. In previous study, indeed, we exhibited that diastereomers of mononuclear (chiral) complexes indicated similar results (namely slight differences) about anisotropic alignment resulting from Weigert effect. In addition, coordination environment of flexible mononuclear Cu(II) complexes was not as suitable for transferring intermolecular interaction from azo-dyes as that of rigid mononuclear Zn(II) complexes. Since cyclohexane possessed by **ML$_1$** is composed of a single bond, it is hardly affected by intermolecular effect [26,27] due to molecular reorientation of **MO**. Because cyclohexane moiety of **ML$_1$** is composed of a single bond, it would be hardly affected by molecular reorientation of **MO**. On the other hand, phenylenediamine of **ML$_2$** is rigid and flat aromatic ring, resulting in its susceptible nature to molecular reorientation of **MO**. Thus, the change of anisotropic parameter *R* would be affected by the difference in the susceptibility of **ML$_1$** and **ML$_2$** to the molecular reorientation of **MO**. In other words, since phenylenediamine possessed by **ML$_2$** is an aromatic ring and a planar shape, it is susceptible to intermolecular effect due to molecular reorientation of MO. As a result, **ML$_2$** is oriented without inhibiting the molecular reorientation of **MO**. However, **ML$_1$** inhibits the molecular reorientation of **MO** [28]. This is related to the magnitude of the change in the anisotropic parameter *R* depicted in Scheme 4. The quality of data (statistical dispersion) and magnitude of optical anisotropy induced are common ranges for that of the recent examples [29]. By using these mechanisms, potential applications can be expected such as chiroptical probes of spectroscopy [30,31] or sensors [32], and chiral materials of nanostructure in oriented ones [32] or surface [33,34].

Scheme 3. Flexibility (or rigidity) of ligands and intermolecular effect from **MO**.

Scheme 4. Molecular orientation and parameter change (proposed mechanism).

5. Conclusions

In summary, we have synthesized two series of new binuclear Schiff base Ni(II), Cu(II), and Zn(II) complexes. One series is the complexes that have flexible cyclohexane moiety on the amine site

(**ML₁**: **NiL₁**, **CuL₁**, and **ZnL₁**) and the other series is the complexes that have rigid aromatic six-membered ring moiety on the amine site (**ML₂**: **NiL₂**, **CuL₂**, and **ZnL₂**) instead of the cyclohexane moiety. We have also prepared their hybrid materials (**ML₁+MO+PVA** and **ML₂+MO+PVA**) as **PVA** cast films. The polarized UV-vis spectra of the hybrid materials after linearly polarized UV light irradiation were measured. From the changes of the anisotropy parameter *R*, it was found that **ZnL₂+MO+PVA** exhibited the highest anisotropic orientation induced among the six materials. In addition, the magnitude of the anisotropic parameter *R* was compared among **ML₁+MO+PVA** and **ML₂+MO+PVA**. As a result, it was found that the orientation of **ML₂**, of which the ligand had many aromatic groups, was induced the most effectively of all the metals. Therefore, the susceptibility of the molecular reorientation by **MO** to the complex through intermolecular interactions leads to enhancement in the anisotropic molecular orientation of the complex. In this way, the change of anisotropic parameter *R* would be affected by the difference in the susceptibility of **ML₁**, which has flexible cyclohexane moiety, and **ML₂**, which has a rigid phenyl group with regard to the molecular reorientation of **MO**. These results also support a mechanism based on intermolecular interaction and emphasize the significance of the rigidity of the ligands even for binuclear complexes for effective receiving such as intermolecular interaction from **MO** (azo-dyes influenced by Weigert effect directly).

References

1. Velema, W.A.; Szymanski, W.; Feringa, B.L. Photopharmacology: Beyond Proof of Principle. *J. Am. Chem. Soc.* **2014**, *136*, 2178–2191. [CrossRef] [PubMed]

2. Xu, Z.; Shi, L.; Jiang, D.; Cheng, J.; Shao, X.; Li, Z. Azobenzene Modified Imidacloprid Derivatives as Photoswitchable Insecticides: Steering Molecular Activity in a Controllable Manner. *Sci. Rep.* **2015**, *5*, 13962. [CrossRef] [PubMed]

3. Wang, L.; Li, Q. Photochromism into nanosystems: Towards lighting up the future nanoworld. *Chem. Soc. Rev.* **2018**, *47*, 1044–1097. [CrossRef] [PubMed]

4. Delaire, J.A.; Nakatani, K. Linear and Nonlinear Optical Properties of Photochromic Molecules and Materials. *Chem. Rev.* **2000**, *100*, 1817–1845. [CrossRef] [PubMed]

5. Grebenkin, S.; Meshalkin, A.B. Wavelength Dependence of the Reorientation Efficiency of Azo Dyes in polymer Matrixes. *J. Phys. Chem. B* **2017**, *121*, 8377–8384. [CrossRef] [PubMed]

6. Natansohn, A.; Rochon, P. Photoinduced Motions in Azo-Containing Polymers. *Chem. Rev.* **2002**, *102*, 4139–4175. [CrossRef] [PubMed]

7. Ichimura, K. Photoalignment of Liquid-Crystal Systems. *Chem. Rev.* **2000**, *100*, 1847–1874. [CrossRef] [PubMed]

8. Sekkat, Z.; Dumont, M. Photoinduced orientation of azo dyes in polymeric films. Characterization of molecular angular mobility. *Synth. Met.* **1993**, *54*, 373–381. [CrossRef]

9. Beaudoin, E.; Abecassis, B.; Constantin, D.; Degrouard, J.; Davidson, P. Strain-controlled fluorescence polarization in a CdSe nanoplatelet–block copolymer composite. *Chem. Commun.* **2015**, *51*, 4051–4054. [CrossRef] [PubMed]

10. Ma, H.; Zhu, M.; Luo, W.; Li, W.; Fang, K.; Mou, F.; Guan, J. Free-standing, flexible thermochromic films based on one-dimensional magnetic photonic crystals. *J. Mater. Chem. C* **2015**, *3*, 2848–2855. [CrossRef]

11. Akitsu, T.; Komorita, S.; Urushiyama, A. Assignment of d-d Transitions of Square Planar [Cu^{II}N$_4$] Complexes Containing Imidate and Amine Ligands by Polarized Crystal Spectra and Angular Overlap Model. *Bull. Chem. Soc. Jpn.* **2001**, *74*, 851–860. [CrossRef]

12. Mande, H.M.; Ghalsasi, P.S.; Navamoney, A. Synthesis, structural spectroscopic characterization of the thermochromic compounds A$_2$CuCl$_4$ [(Naphthylethylammonium)$_2$CuCl$_4$]. *Polyhedron* **2015**, *91*, 141–149. [CrossRef]

13. Sakai, H.; Safvan, C.P.; Larsen, J.J.; Hilligsoe, K.M.; Hald, K.; Stapelfeldt, H. Controlling the alignment of neutral molecules by a strong laser field. *J. Chem. Phys.* **1999**, *110*, 10235–10238. [CrossRef]

14. Ohshima, Y.; Hasegawa, H. Coherent rotational excitation by intense nonresonant laser fields. *Int. Rev. Phys. Chem.* **2010**, *29*, 619–663. [CrossRef]

15. Akitsu, T.; Itoh, T. Polarized spectroscopy of hybrid materials of chiral Schiff base cobalt(II), nickel(II), copper(II), and zinc(II) complexes and photochromic azobenzenes in PMMA films. *Polyhedron* **2010**, *29*, 477–487. [CrossRef]

16. Aritake, Y.; Takanashi, T.; Yamazaki, A.; Akitsu, T. Polarized spectroscopy and hybrid materials of chiral Schiff base Ni(II), Cu(II), Zn(II) complexes with included or separated azo-groups. *Polyhedron* **2011**, *30*, 886–894. [CrossRef]

17. Aritake, Y.; Akitsu, T. The role of chiral dopants in organic/inorganic hybrid materials containing chiral Schiff base Ni(II), Cu(II), and Zn(II) complexes. *Polyhedron* **2012**, *31*, 278–284. [CrossRef]

18. Yamazaki, A.; Akitsu, T. Polarized spectroscopy and polarized UV light-induced molecular orientation of chiral diphenyl Schiff base Ni(II) and Cu(II) complexes and azobenzene in a PMMA film. *RSC Adv.* **2012**, *2*, 2975–2980. [CrossRef]

19. Ito, M.; Akitsu, T.; Palafox, M.A. Theoretical interpretation of polarized light-induced supramolecular orientation on the basis of normal mode analysis of azobenzene as hybrid materials in PMMA with chiral Schiff base Ni(II), Cu(II), and Zn(II) complexes. *J. Appl. Solut. Chem. Model.* **2016**, *5*, 30–47.

20. Takase, M.; Akitsu, T. Linearly polarized light-induced anisotropic orientation of binuclear Ni(II), Cu(II), and Zn(II) Schiff base complexes including or without methyl orange in PVA. In *Polymer Science Book Series—Volume #1: "Polymer Science: Research Advances, Practical Applications and Educational Aspects"*; Formatex Research Centre: Badajoz, Spain, 2016; pp. 301–308.

21. Sheldrick, G.M. A short history of shelx. *Acta Crystallogr. Sect. A* **2008**, *64*, 112–122. [CrossRef] [PubMed]

22. Schellman, J.; Jensen, H.P. Optical spectroscopy of oriented molecules. *Chem. Rev.* **1987**, *87*, 1359–1399. [CrossRef]

23. Norden, B.; Todger, A.; Dafforn, T. *Linear Dichroism and Circular Dichroism A Textbook on Polarized-Light Spectroscopy*; RSC Publishing: Cambridge, UK, 2010.

24. Yamazaki, A.; Kominato, C.; Matsuoka, S.; Watanabe, Y.; Akitsu, T. Polarized Electronic Spectra of 3 Components Organic/ Organic/ Inorganic Hybrid Materials of Chiral Schiff Base Cu(II) Complex, Azobenzene, and Viologens. In *Integrating Approach to Photofunctional Hybrid Materials for Energy and the Environment*; Nova Science Publishers, Inc.: Hauppauge, NY, USA, 2013; Chapter 6, pp. 125–138.

25. Yamazaki, A.; Akitsu, T. Polarized Spectra of Diastereomers of Schiff Base Ni(II) and Cu(II) Complexes and Azobenzene for Chiral Molecular Recognition in Organic/Inorganic Hybrid Materials. In *Magnets: Types, Uses and Safety*; Nova Science Publishers, Inc.: Hauppauge, NY, USA, 2012; Chapter 2, pp. 51–67.

26. Takano, H.; Takase, M.; Sunaga, N.; Ito, M.; Akitsu, T. Viscosity and intermolecular interaction of organic/inorganic hybrid systems composed of chiral Schiff base Ni(II), Cu(II), Zn(II) complexes having long ligands, azobenzene and PMMA. *Inorganics* **2016**, *4*, 20–29. [CrossRef]

27. Van der Asdonk, P.; Kouwer, P.H.J. Liquid crystal templating as an approach to spatially and temporally organise soft matter. *Chem. Soc. Rev.* **2017**, *46*, 5935–5949. [CrossRef] [PubMed]

28. Statman, D.; Janossy, I. Study of photoisomerization of azo dyes in liquid crystals. *J. Chem. Phys.* **2003**, *118*, 3222. [CrossRef]

29. Akitsu, T.; Yamazaki, A.; Kobayashi, K.; Haraguchi, T.; Endo, K. Computational Treatments of Hybrid Dye Materials of Azobenzene and Chiral Schiff Base Metal Complexes. *Inorganics* **2018**, *6*, 37. [CrossRef]

30. Moletti, A.; Coluccini, C.; Pasini, D.; Taglietti, A. A chiral probe for the detection of Cu(II) by UV, CD and emission spectroscopies. *Dalton Trans.* **2007**, 1588–1592. [CrossRef] [PubMed]

31. Agnes, M.; Nitti, A.; Griend, D.A.V.; Dondi, D.; Merli, D.; Pasini, D. A chiroptical molecular sensor for ferrocene. *Chem. Commun.* **2016**, *52*, 11492–11495. [CrossRef] [PubMed]

32. Caricato, M.; Leza, N.J.; Roy, K.; Dondi, D.; Gattuso, G.; Shimizu, L.S.; Griend, D.A.V.; Pasini, D. A Chiroptical Probe for Sensing Metal Ions in Water. *Eur. J. Org. Chem.* **2013**, 6078–6083. [CrossRef]

33. Caricato, M.; Sharma, A.K.; Couluccini, C.; Pasini, D. Nanostructuring with chirality: Binaphthyl-based synthons for the production of functional oriented nanomaterials. *Nanoscale* **2014**, *6*, 7165–7174. [CrossRef] [PubMed]

34. Caricato, M.; Delforge, A.; Bonifazi, D.; Dondi, D.; Mazzanti, A.; Pasini, D. Chiral nanostructuring of multivalent macrocycles in solution and on surfaces. *Org. Biomol. Chem.* **2015**, *13*, 3593–3601. [CrossRef] [PubMed]